

# Synchronised WindScanner Field Measurements of the Induction Zone Between Two Closely Spaced Wind Turbines

Anantha Padmanabhan Kidambi Sekar, Paul Hulsman, Marijn Floris van Dooren and Martin Kühn

December 18, 2023

---

## Reviewer 1

The authors present measurements of the induction zone of a wind turbine. The measurements were acquired by two Doppler lidars, that scanned in a synchronous mode a horizontal plane, at the hub height of a 3.5 MW wind turbine, that extended up to 0.8 D upstream. The conduction of field campaigns using multiple Doppler lidar is a challenging task. The authors provide a thorough description of the installation and the alignment of the wind lidars, as well as an investigation of the magnitude of the errors in the measuring setup. Using the acquired wind measurements, the spatial characteristics of the induction zone are examined during four periods when the inflow of the wind turbine examined was characterised by free flow, fully waked or partially waked conditions. The overall manuscript is well written and well structured. However, I think that there are some parts that should be clarified and explained better, before the article is ready for publication. I am highlighting these points in the list below.

*We thank the reviewer for their critical assessment of our work. In the following we address their concerns point by point. We hope these changes will positively benefit the manuscript. Comments to the reviewer points are made in blue while modifications to the manuscript are shown in red.*

Based on the comments of Reviewers 1, 2 we have summarised the major changes in the revised manuscript below:

- Expanded the site characterisation section with the topography and the presence of flow blockage (treeline) in between the two turbines and the discussion section to include the effects of the topography and treeline as a possible explanation for our measured flow features and a discussion on how to decouple the terrain effects from the rotor aerodynamic effects.
- Updated the LES results section with an analysis of the statistical uncertainty of the measurements.
- Expanded the LES Results section to include the rationale behind our assumption of the vertical velocity on the Standard Uncertainty Propagation (SUP) and its impact on the width of error bars. The discussion section has been updated to include the significance of our results based on the SUP assumptions and suggestions for future measurements with a third synchronised lidar.
- The conclusion section has been reworked substantially to include a description of our measurements, measured flow features, a summary of the uncertainty analysis and summary

of challenges in conducting field measurements for obtaining validation data for numerical models.

---

## Main Comments

**Comment 1:** The authors present four data sets of induction zone measurements, which correspond to cases where the inflow of a utility-scale wind turbine is characterised by free, waked and partially waked conditions. There is a thorough description of the observed spatial features of the flow, but there is a lack of scientific conclusions. The interaction of the induction zone with the wake flow is something to be expected. My recommendation to the authors is to present what do we learn from the results of this study. In the last sentence of the Conclusions sections they write “A preliminary evaluation of the engineering models of the induction zone indicates that the models do not completely capture the complex flow behaviour and turbine interactions”. I could not find a discussion of this topic in the manuscript for the case of the waked inflow. Figure 12 shows the induction zone for a free flow, but when the authors write “turbine interactions” I understand they did an evaluation of engineering models of the induction zone in waked conditions.

**Reply:**

The objective of the work was first to use the unique fast scanning capabilities of the WindScanner systems and quantify the measurement errors due to the limitations of our experimental setup. We were able to calculate the magnitude of errors using a virtual lidar in LES approach and successfully characterised the induction zone for multiple inflow scenarios. The main conclusion that we could draw from our study is the complexity of setting up synchronised lidar measurements, difficulty in quantifying the effects that are seen in field measurements due to limitations in our measurement setup (no third lidar), the additional considerations needed to characterise the induction zone behaviour based on error analysis and therefore how one should interpret the observed flow fields. We believe this to be an important contribution as field data is usually considered as “ground truth” and is demanded as a reference for qualitative and quantitative validations of numerical flow development models. Therefore, we have strived to provide a thorough description of the site, lidars, measurements and their associated uncertainties for comprehensive traceability of our work in addition to making the lidar dataset available on request for future studies and validation attempts.

Indeed the observed spatial flow features such as induction - wake interaction and the induction zone behaviour during wake steering are expected phenomena. However, the experiments are, to the author’s knowledge, the first high-resolution measurements of the induction zone - wake interaction for utility-scale turbines.

On the topic of turbine interactions, we had evaluated the coupled FLORIS induction zone model for the waked and partially waked cases but had not presented them in the paper due to the inability of the model to capture the flow field behaviour that was expected after the poor model performance in the undisturbed induction zone. We will therefore remove our statement in the conclusions and expand the discussion section that an analysis was performed but not shown in the paper.

We have updated the conclusion section based on our answer above.

**Comment 2:** Figure 1 presents a photograph of the landscape where the measurement campaign took place. There we can see that the topography of the area between the two wind turbines is not homogeneous. There is a tree fence which is located in the vicinity of the WT1 wind turbine and extending towards the meteorological mast, and furthermore a crop field between the wind turbines WT1 and WT2. The authors don't describe in detail the physical characteristics of these features and don't discuss what if there is, or not, an impact of these features on the flow. I think that this is important, since it can partially explain the features of flow presented in Figs 6, 10, 13 and 15. For example, in Fig. 10 (c) the induction zone is seen to be symmetric right in-front of the rotor plane, but it gets asymmetric as the upwind distance increases. Why should this happen? Have the authors acquired any measurements or have they performed an LES study of the flow (where the variations of the terrain features were taken into consideration) while both wind turbines were not operating?

**Reply:** We acknowledge that we did not discuss the site layout in detail. The induction zone of onshore wind turbines can be incorrectly estimated using observations if the effects of nonuniform terrain on the flow are not carefully considered. This non-uniformity could be a result of the changing elevation upstream of the turbine or as pointed out, through the presence of a high tree line. The impact of terrain on the induction zone have been studied through simulations [17] and experiments [13]. For instance, Mikkelsen et al., [13] in their dual-WindScanner lidar measurements at the DTU Riso site measured a vertical velocity of 1 m/s in the induction zone which was attributed to the sloping terrain upstream of the turbine.

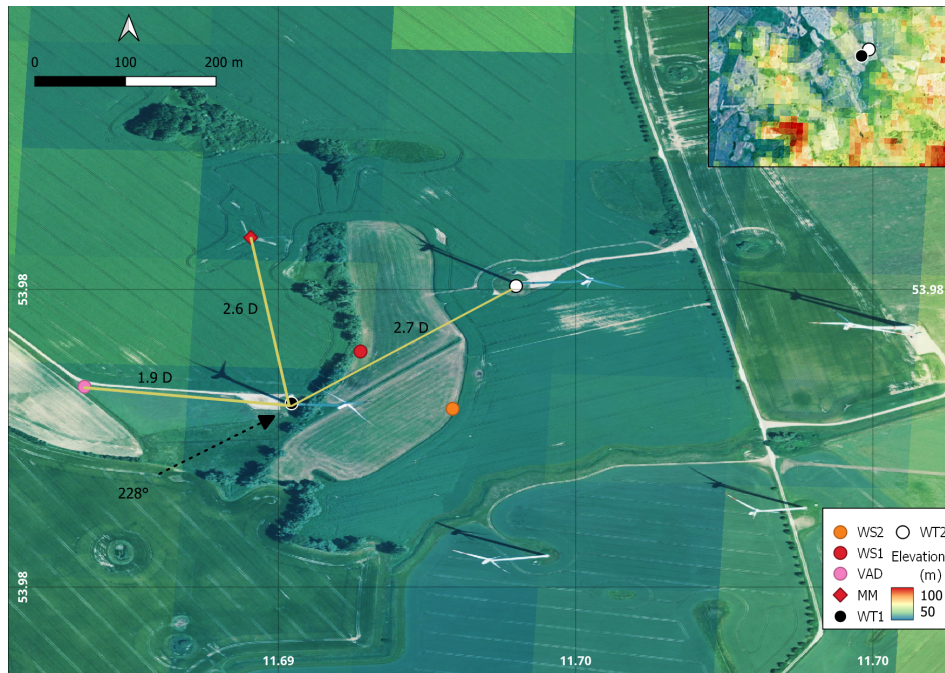


Figure 1: The wind park and measurement layout at Kirch Mulsow with elevation contours. A zoomed out image of the site is shown in the top right corner illustrating the hills present upstream of the wind park. Here WT1, and WT2 refer to the upstream and downstream turbines, MM and VAD are met mast and the VAD lidar while WS1, WS2 refer to the WindScanners.

We provide a more detailed description of the site, as illustrated in Fig. 8. The elevation data was obtained with a resolution of 200m maintained by the German Ministry of Cartography and Geodesy [3]. While the elevations at the locations of the two turbines WT1, WT2 are approximately 52 m, abrupt elevation changes are seen upstream notably the presence of a small hill with an elevation of 105 m 22 D upstream of WT1 along the predominant wind direction of 228°, creating a slope of 1.09° towards the two turbines. The village of Garvensdorf with its farmhouses was approximately 1200 m upstream of WT1.

We also note the presence of tree lines and small clumps of forested terrain. As rightly pointed out, a treeline exists between WT1 and WT2 extending towards the met mast with a height of approximately 15 m-20 m estimated from pictures made during installation while other tree lines and clumps of forested area are present at various upstream positions along the 228° sector. Further analysis of the measurements from the same site was done by Hulsman et al. [10] who showed a non-negligible effect of the tall tree line by comparing the met mast and the VAD lidar data at 100 m elevation. However, the comparison is not directly transferable in our sector of interest due to the orientation of the VAD lidar and the met mast but provides enough evidence of the perturbation of the flow by the same treeline. This is consistent with literature where treelines acting as windbreaks have been shown to perturb the vertical flow profile high above the treeline [7, 19].

Therefore, terrain effects, in particular the treeline could have potentially influenced the induction zone flow. Furthermore, these could have also impacted the WindScanner measurements, in particular, the assumption of  $w = 0$  m/s for the dual-Doppler reconstruction which could have influenced the measurement results shown in this paper.

However, we could not quantify the magnitude of these terrain effects on the flow and the lidar measurements. We could not acquire synchronised measurements when both the turbines were non-operational, which would have provided insights into the flow behaviour due to terrain. We acknowledge that a high-resolution LES study with a terrain map could have been used to isolate the flow behaviour due to terrain and the turbine influence. However, the LES runs in our study were intended to study the lidar measurement accuracy and therefore were initialised with a roughness length as a proxy for the terrain complexity.

We have updated the test site characterisation section, and also updated the corresponding results discussion section with the potential impact of the site orthography on the measured flow features.

**Comment 3:** Following the comment above, in the abstract and the conclusions it is stated that the measurements presented in this article reveal a horizontal asymmetry of the induction zone which the authors claim that it is due to the vertical shear. This statement is based on the observed characteristics of one case (Case 1), with a shear exponent equal to 0.21. On which basis the authors support that this shear exponent is strong enough in order to induce a horizontal asymmetry? And how can they decouple the observed horizontal asymmetry from potential spatial variations of the horizontal flow due the heterogeneity of the terrain?

**Reply:** Ideally, we would have liked to show at least two undisturbed inflow cases, with a range of shear (or at the least strong and weak), with similar inflow and turbine operational conditions and measured with the same instrumentation. This was impossible in the limited amount of time we could perform measurements. This is the limitation of the study as the outcomes were based on small datasets which is just a small portion of the operational states of the wind turbine.

Bastankah et al, [2], in their wind tunnel experiments noted a "slight asymmetry with respect to rotor

axis” with a shear exponent of 0.17 and attributed the reason to the sheared inflow. Our argumentation followed this work and the stronger shear exponent (0.21) that was present during the measurements. However, as discussed earlier, we had discounted the effect of terrain on the flow and the measurements. Performing multiple LES runs with a flat terrain and the map of the terrain with increasing values of vertical shear can potentially decouple the effects of the terrain and the shear on the flow and identify the driving factors behind the asymmetry and provide a strong explanation for our measurements.

We have expanded the discussion of our results mentioned above to include the potential impact of the terrain characterisation on our measurements.

**Comment 4:** I think that the error values that are used in Sect 3.1, concerning the line-of-sight (0.1 %) and the pointing accuracy (0.1 deg) are rather low. Regarding the line-of-sight the authors use as a reference the work of Pedersen and Courtney 2021 to support the choice of the 0.1 % value. First, the value reported in that study concerns a cw Doppler lidar, but not the Doppler lidars used here. And second, I guess that the line-of-sight error is dependent also on the probe length. Regarding the pointing accuracy, this will be dependent on the scanning speed. I think that the authors should address these points in the “Discussion” section.

**Reply:** We acknowledge the points made by the referee regarding the line-of-sight and pointing errors. For continuous-wave lidars, the error will be dependent on the probe length which scales quadratically with the focus distance. The work of Pedersen and Courtney [15] suggests a 0.1% error, but as pointed out was with a different lidar system in a highly controlled environment. van Dooren et al ([21]), used the same WindScanner lidars in a wind tunnel study and quantified the error against a hot wire anemometer with a mean average error metric less than 2 %, dependant on the turbulence intensity of the inflow in their set up. The probe length in this study was in the order of 13 cm and 13.9 cm for the two WindScanners respectively. For our field measurements, where probe lengths were in the order of 6.75 m to 27.75 m, an increase in the error will be expected. One way to estimate this error would have been to set up a field measurement, focus the WindScanners with similar focus distances next to a sonic anemometer to obtain representative probe lengths, project the sonic measurements into the line-of-sight and compare the accuracy of the two systems. However, such a campaign was not executed before this study was conducted.

Indeed, the pointing accuracy will be dependent on scanning speed. We had chosen a sinusoidal motion pattern as this could be achieved by continuously rotating the two prisms in one direction only. Sinusoidal scanning therefore reduced the acceleration of the scan head reducing induced vibrations and eliminating the scan reset time. The two prisms in the WindScanner are controlled through a programmable multi-axis motion controller (PMAC), whose input is the angular position of the prisms calculated beforehand for a particular scan trajectory. Depending on the scanning trajectory, speed and the limitations of the system, it might be the case that the prism might not reach its intended angular position before performing a movement to the next measurement location. The WindScanner data stream captures the actual angular position along with the commanded motion positions. Figure 2 illustrates this difference ( $\Delta\theta_{M1}, \Delta\theta_{M2}$ ) for the two steering motors for three consecutive horizontal plane scans from the presented measurement setup. For both motors, the values of  $\Delta\theta_{M1}, \Delta\theta_{M2}$  did not exceed  $0.1^\circ$ , except for 16 points (0.12%) in each full measurement. These points were located on the very edges of the measurement plane and could not be fully eliminated. As more than 99 % of the measurement points showed an average pointing error of less than  $0.1^\circ$ , we report this number.

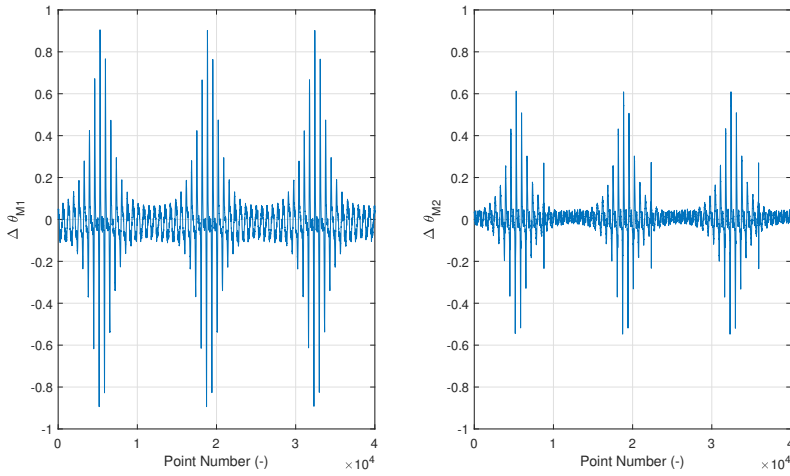


Figure 2: Angular difference between the commanded and actual motor positions for the two steering motors M1 and M2.

We have updated the discussion section with the explanation:

We note that the error in  $v_{los}$  of 0.1 % might be low compared to our measurements. The work of [15] suggested a 0.1% error in a highly controlled environment. [21], used the same WindScanner lidars in a wind tunnel study and quantified the error against a hot wire anemometer with a mean average error metric less than 2 % in their set-up. However, the probe lengths in this study were of the order of 13 cm. For our field measurements, where probe lengths were in the order of 6.75 m - 27.75 m, an increase in the error is expected. Further measurements are required, for example, by focusing the lidars against a sonic anemometer with representative probe lengths into the lidar line-of-sight to obtain a representative  $e_{v_{los}}$ .

**Comment 5:** Section 3 presents the results of the virtual Windscanner evaluation using LES. According to the LES the largest values of the “w” component are equal to +/- 0.8 m/s (by taking into consideration the contours of Fig.6 and the inflow free wind speed at the hub height (7.7 m/s). However, for the estimation of the propagated uncertainty a constant vertical component is assumed, with a varying magnitude for each of the cases. Specifically, in Sect. 3.2.1 “w” is equal to 0.2 m/s while in Sects. 3.2.2 and 3.2.3 “w” is equal to 1.0 m/s. Can the authors comment on the selection of those values?

**Reply:** We acknowledge that the reasoning behind the choice of  $w$  velocities for the propagated uncertainty calculations was not detailed in the paper. In the LES analysis, the simulated data provided an accurate value of the local  $w$  component variation inside the scanning area. This local  $w$  velocity was subsequently used to calculate the propagated uncertainties providing a methodology to investigate the lidar error inside the LES. However, in the free field, we did not have any measurements of the local  $w$  component. Therefore, an assumption of a constant  $w$  was required for the Standard Uncertainty Propagation (SUP) methodology. For the full wake and partial wake cases, a value of  $w = 1$  m/s was assumed, similar to the wind tunnel experiments of van Dooren et al [20]. For the undisturbed inflow



case, the vertical velocity would be only dominated by the temperature flux between the ground and the air, and therefore a conservative value of  $w = 0.2$  m/s was chosen based on the weakly stable conditions during the measurements.

The assumption of constant  $w$  velocities in the measurement plane for SUP calculations will have a significant impact on our results. Due to this assumption, the errors would be overestimated at locations where the local  $w$  component would be low, for instance, the most upstream part of the scan where the aerodynamic influence of the rotor on the flow would not be felt by the wind field. To illustrate this we plot the variation of  $e_u$  and  $e_v$  in the scanning area for the LES case with an assumption of  $w = 1$  m/s in Figure 7.

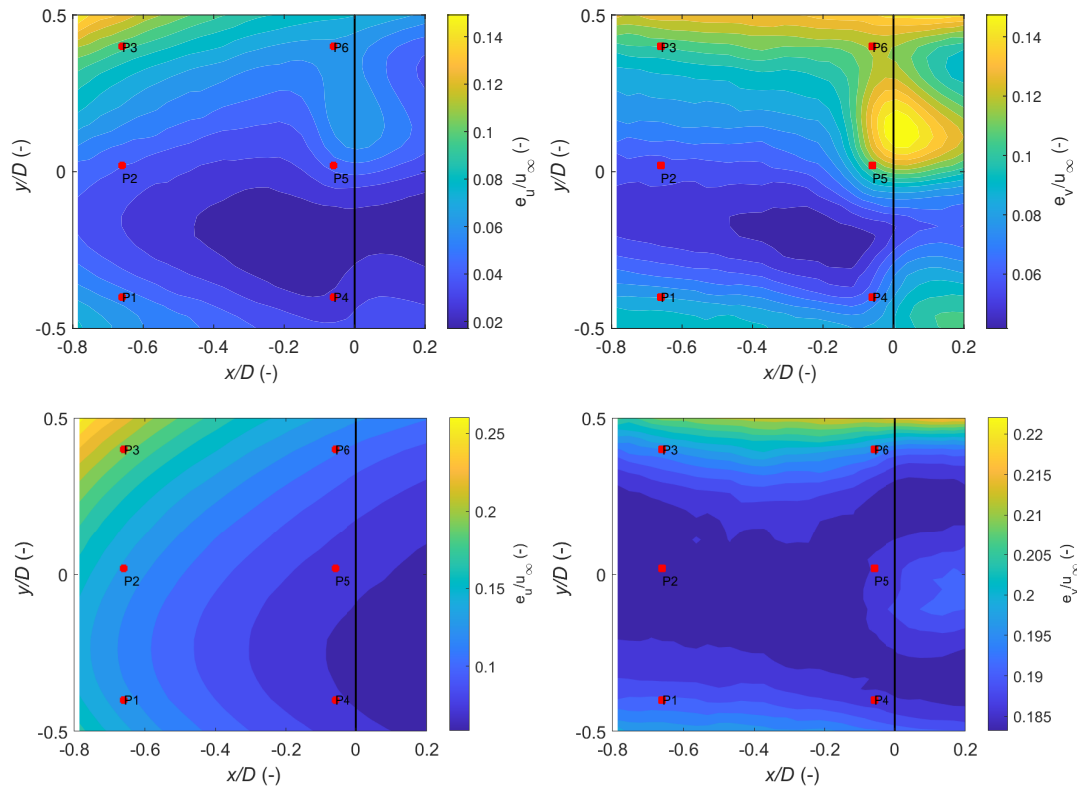


Figure 3: Variation of  $e_u$  and  $e_v$  in the scanning area using the local  $w$  component from the LES (first row) and the assumption of  $w = 1$  m/s (second row).

The comparison of  $e_u$  and  $e_v$  for the two methods indicates a couple of things. Firstly, assuming constant  $w$  velocities on the scanning area masks the velocity reconstruction error that is dependent on the flow dynamics, especially close to the rotor. Secondly, the magnitude of  $e_u$  and  $e_v$  for the constant  $w$  velocity case is substantially larger than the errors estimated using the local  $w$  velocities. The consequence of this is that the presented error bars in Figures 11, 14, 16 and 17 of the original manuscript are conservative and as pointed out by Reviewer 2, leads to difficulties in the interpretation and significance of the results. A possible workaround would have been to use a third synchronised lidar that would eliminate the assumption of vanishing vertical velocity, however, a third system was not available for measurements. We acknowledge this unavoidable limitation of our measurement setup and have made the following changes in the manuscript.

We have expanded the LES section with the results presented in Figure 7 for the constant  $w$  velocity assumption and extended the discussion section, highlighting the assumption and its impact on the significance and interpretation of the measurements.

## Specific Comments

---

**Comment 1** — Lines 10 – 12: The authors write: “The measurements revealed more evidence of horizontal asymmetry of the induction zone owing to vertical wind shear under undisturbed inflow conditions”. Why do the authors write “revealed more evidence” here, since it is the first time where they mention the horizontal asymmetry of the induction zone?

**Reply:** We acknowledge that the phrasing of this sentence was not clear in the abstract. Based on the comments of both reviewers, we have rephrased this sentence to the following:

The measurements revealed the existence of a horizontal asymmetry in the induction zone possibly due to a combination of the rotor and terrain effects under undisturbed inflow.

**Comment 2** — Lines 14 – 15: The authors write: “We observed that the downstream turbine induction zone during wake steering depended on the direction of the wake steering...”. Isn’t this an obvious statement?

**Reply:** Yes, this is an obvious statement. At the end of the sentence, we mentioned that the “lateral movement of the deflected wake could be measured”. To our knowledge, this was the first time, the lateral velocities in the deflected near wake were measured in field experiments. Therefore, we have modified this sentence to the following:

We observed the downstream turbine induction zone during wake steering while the lateral movement of the deflected wake could be measured for the first time in the free field.

**Comment 3** — Lines 105 – 106: What was the purpose of equipping the mast with a gas analyser?

**Reply:** The Irgason device is an eddy covariance system which combines both an infrared gas analyzer (IRGA) and a 3D sonic (SON) anemometer combined into a single sensor. For characterising the atmospheric stability, the Obhukov length was used. Therefore, flux measurements were carried out at the met mast at three heights, 2 m, 6 m and 60 m. Additional temperature and relative humidity probes were installed to calculate the mean air density for the moisture correction of sensible and latent heat fluxes. A more detailed description of the method for estimating stability from the Irgason is detailed in Bromm et al., [6]. We have added the following to the text:

More details on the derivation of the Obhukhov length from the Irgason are detailed in [6].

**Comment 4** — Line 110: What was the spatial resolution of the inflow lidar?

**Reply:** The pulse length of the inflow lidar was 25 m. This information has been updated in the revised manuscript.

The inflow lidar was performing VAD scans with a elevation angle of  $75^\circ$  and with range gates set from 50 m to 840 m with a spacing of 5 m and a pulse length of 25 m.



**Comment 5** — Line 146, Eq.5: Please describe what is denoted by “ $\mathbf{x}$ ”.

**Reply:** The term  $\mathbf{x}$  denotes the spatial position vector of the measurement point in space. We have updated the text to the following:

The measured line-of-sight velocities of a cw lidar at the position  $\mathbf{x} = (x, y, z)$ ,  $v_{\text{los}}(\mathbf{x})$  can be mathematically expressed as the convolution of the wind vector  $\mathbf{u}(\mathbf{x})$  projected along the laser beam direction and the volume averaging function:

**Comment 6** — Line 151: The effective radius is an important parameter for the operation of a cw Doppler lidar since it determines the spatial resolution of the lidar. How is the value stated here (56 mm) determined?

**Reply:** We did not conduct any experiments to calculate the effective radius. The effective radius of the WindScanners were reported by DTU Wind Energy who developed the WindScanner systems.

**Comment 7** — Line 169: What is meant with the term “greedy controller”?

**Reply:** The term “Greedy Controller” is used here to describe the control strategy when both the turbines were operated to extract maximum power, i.e., no wake steering was performed when this controller was active. We have rephrased this sentence to the following:

In this sector, active wake steering was performed by toggling between two unique wake steering controllers and one greedy controller where no wake steering is performed, each operational for 35 minutes.

**Comment 8** — Line 172 – 173: How were the group of horizontal planes averaged? Where the measurements grouped based on their position in a grid?

**Reply:** We have described the post-processing of the measurement data in the beginning of Section 3, Results but have moved the text to Section 2.2.1.

For visualisation, the longitudinal and lateral velocities are interpolated using a cubic interpolation scheme onto a uniform grid with a spacing of 10 m. We rotated all measurements in the global reference frame into the main wind direction at the met mast hub height.

**Comment 9** — Line 175, Table 2: The authors present in Table 2 a list of different types of errors along with a qualitative characterisation of their impact. I think that this qualitative characterisation rather than general, it depends a lot on the measuring configuration and features of the measured flow. Therefore, I suggest that the authors should either discuss why the impact of these errors are general or mention that this characterisation concerns the specific measuring campaign. For example, the assumption of zero vertical component is probably not high over offshore areas. Furthermore, maybe this table is more part of the “Results” than of the “Methods”.

**Reply:** Agreed that the impact and magnitude of the errors from different sources are highly site-specific. However, we prefer to keep the table at the beginning as it would allow the reader to have an overview of the different errors before reading through the section. To make our table specific for our particular setup, we have modified the following text to:

For this particular measurement setup, the various lidar errors, their impact and their analysis methodology are tabulated in Table 2.

**Comment 10** — Line 186: Why is the maximum distance of the cw lidars used equal to 300 m?

**Reply:** Continuous-wave systems have an inherent maximum range (on the order of a few hundred meters), beyond which it is impossible to focus the beam, because of diffraction [8]. Furthermore, the maximum range of the cw lidars has been specified as 300 m as the measurement volume extends beyond 30 m after this range. This definition of maximum range follows the reasoning of the smaller 3” WindScanners first developed by DTU, whose maximum range was 150 m after which the probe volume extended beyond 30 m.

**Comment 11** — Line 189: “This effect is most severe for measurements at the wake edges, . . .” Please add that this statement concerns this study.

**Reply:** We agree with this statement. The text has been amended to:

This effect concerns our study as is most severe for measurements at the wake edges, as the measurement volume extends from inside the wake to the freestream, and for measurements very close to the downstream turbine WT2, as the measurement volume would extend partially into the turbine wake.

**Comment 12** — Lines 202 – 203: What is meant with the term “effective intersection diameter”?

**Reply:** Giyanani et al [9] define effective intersection diameter for a synchronised WindScanner system as the diameter of a sphere circumscribing the location of the laser beams at the focal point. The effective diameter therefore describes the sphere within which the laser beams are expected to intersect at a particular measurement point.

**Comment 13** — Lines 213 – 218: I think that the authors should refer here to already published articles that have investigated the impact of the measuring position to measuring errors in a dual lidar measuring configuration, such as:

Peña A, Mann J. Turbulence Measurements with Dual-Doppler Scanning Lidars. Remote Sensing. 2019; 11(20):2444. <https://doi.org/10.3390/rs11202444> Please note that I am neither the author nor the co-author of the above publication.

**Reply:** We have added relevant references to the paper of Pena and Mann [16] along with the work of Stawiarski et al [18] and van Dooren et al [20] to this section.

**Comment 14** — Lines 231 – 234: Eqns. 7 and 8 assume that the uncertainty terms are uncorrelated. Please add this assumption.

**Reply:** Agreed. We have added the assumption of small errors and the zero correlation between errors for SUP to the text.

**Comment 15** — Line 244. What are the unfavourable conditions that the authors refer to? Please elaborate. And what was the impact of the lower availability on the spatial distribution of the measurements? Were they certain areas with systematically lower data availability values than others?

**Reply:** The majority of the unfavourable conditions were due to periods of rain which impacted our measurements. The spatial availability distribution was dominated by the presence of the wind turbine nacelle and the spinning blades that systematically reduced data availabilities close to and behind the rotor. We have modified the text to the following:

We noticed that many measurements were also affected by unfavourable conditions such as rainfall and lower availability of aerosols to backscatter the laser beam. For operational safety reasons, the WindScanners were operated only with on-site personnel supervision. The measurements were further influenced by the presence of the wind turbine nacelle and the rotating blades that would systematically reduce data availability in the scan region.

**Comment 16** — Line 261. What was the agreement between the power law model and the measurements?

**Reply:** Figure 4 illustrates the averaged vertical wind speed distribution along with the power law fit for the full wake case. In general, a good fit is observed between the measurements and the fit with minor discrepancies noted at the lower and upper parts of the rotor due to the nature of the terrain. Also note that for case 2,3,4, the VAD lidar measurements are influenced by the induction zone of WT1 due to the small separation of  $1.9 D$ .

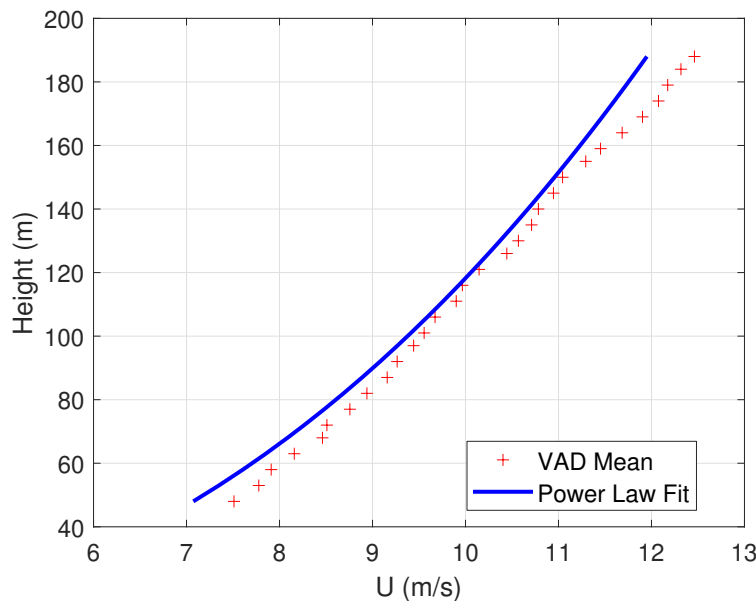


Figure 4: Averaged measurements of the VAD lidar during the occurrence of the full wake case illustrated along with the power law fit.

Furthermore, no flow events such as low level jets which could have impacted our measurements were detected during the investigated measurement periods.

**Comment 17** — Line 306, Figure 6 (top row, right), why does the distribution of the “ $w$ ” component is tilted in respect to the wind turbine rotor?

**Reply:** The tilted / shifted distribution of the  $w$  component could be attributed to the 20 m hub height difference between the upstream and downstream turbines, similar to the field campaign operating in highly veered wind flow that is displacing the wake.

**Comment 18** — Line 310: The authors state that there is “an excellent agreement between the LES and the virtual WindScanner...” I think that this is subjective statement. The author should

explain why they think that there is a good agreement between the two. Especially when in the next sentence it is stated that there are deviations between the virtual lidars and the LES.

**Reply:** We agree that the comparison between the LES and virtual WindScanner profiles is subjective. Here, we wanted to describe that the spatial plots of the 2D velocity reconstructions between LES and WindScanner simulations are similar in a qualitative way, showing that the WindScanner could capture the dominant flow structures with the reference LES wind field such as the flow expansion at the rotor tips. Therefore, we have rephrased the text to:

A good qualitative agreement between the LES and the virtual WindScanner resolved  $u, v$  profiles are noted at most parts of the scanning area. The simulations reveal that the WindScanners can capture the spatial features in the flow such as the wake rotation and flow expansion at the rotor tips.

**Comment 19** — Lines 316 – 335. The authors state that Fig 7. shows that error in “u” is at larger the WT2 rotor plane. However, from the contour plot this is not obvious. For example, the error in P2 is similar to the one at P5 and higher than the P6. Furthermore, the maximum error in the “v” component when  $y/D > 0$  looks that is higher than 14%.

**Reply:** The u component error was stated to be large at the rotor plane at locations where high local  $w$  velocities were present. This can be seen in the seen in Fig.06 top right where the spatial variation of the vertical velocity is shown. The error in P2 and P5 are similar (4.2 % and 4.6 %) due to the similar  $w$  velocities while at P6, the u component error is 6.7 % owing to the larger local  $w$  component present here.

For comparative purposes, we presented the colour axes for both  $e_u$  and  $e_v$  up to 0.2. We have modified the colour limits of this plot in the revised manuscript where it is clear that the maximum value of  $e_v$  at  $y/D > 0$  is 15%.

**Comment 20** — Figure 8. It is very difficult from the colour of the bars to identify the contribution of each error. Can you please choose better colours?

**Reply:** We have updated the figure and assigned a separate colour for the eight error terms for easier visualisation.

**Comment 21** — Line Figure 12 presents the velocity deceleration of the longitudinal wind speed along centre of the rotor. The figure presents that the model based on the 1D Vortex sheet theory fails to reproduce the observed wind characteristics. I am wondering to which extent this is observed due to the model or due to a non-optimum selection of the free wind speed and of the induction zone factor. Have the authors tried to estimate the free wind speed and the induction zone from the Windscanner measurements?

**Reply:** The authors agree with the reviewer that an improper selection of induction factor will have a substantial influence on the modelled flow deceleration. We had indeed investigated estimating  $u_\infty$  and the axial induction factor from the measurements following the work of Borracino et al [4] with the 1-D vortex sheet theory. A negligible difference was seen between the measured and modelled rotor axis velocity deceleration and hence was not reported in the paper.

The most likely reason for the discrepancy is a bug in the coupling between the induction zone models and the wake models in FLORIS. This reasoning is supported by the good agreement between the standalone induction zone models that are used in the coupling and the field measurements.

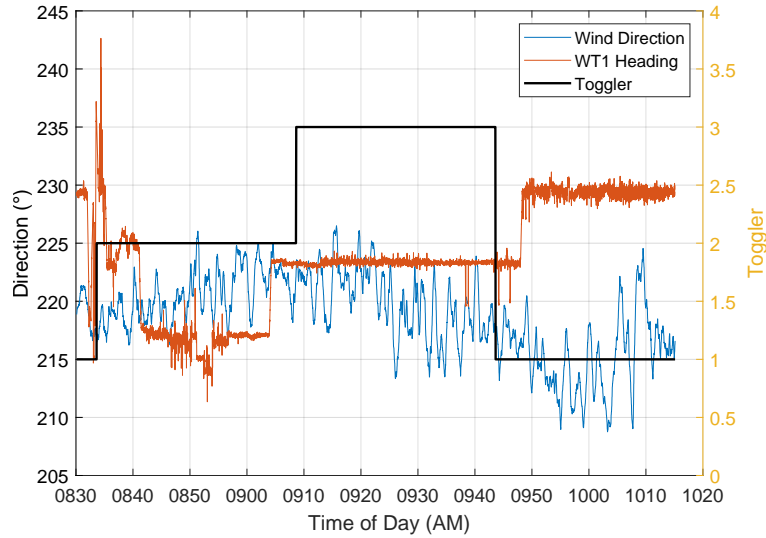


Figure 5: Wind direction from the met mast and WT1 heading on 25.02.2021. The period from 09:45AM to 10:15AM UTC was when the 12.8° yaw offset case was recorded.

**Comment 22** — Line 450. Figure 15 presents the longitudinal component of the wind measured for two different yaw misalignment angles. I can understand the spatial distribution of the “u” component, where the trace of the wake propagates mainly at the region where  $y/D < 0$ . On the other hand when the yaw misalignment of the WT1 is equal to 12.8 degrees then wake tract is in the region where  $y/D > 0$ . However the direction of the propagation of the wake seems strange. I would expect that the wake should move upwards, but from the measurements it looks that it is moving downwards. Can the authors comment on this?

**Reply:** For the 12.8° yaw offset case, the spatial distribution of the longitudinal component seems to indicate that the wake was deflected towards  $y/D \geq 0$ , but closer to the rotor deflects downwards. This could be possibly because of how the measurements were chosen for analysis. The WindScanner was performing measurements when the wind direction was aligned with the two turbines. The mean wind direction for the 12.8° case was 217° already creating an offset as both the turbines are not completely aligned, as in the other three cases. Furthermore, the standard deviation of wind direction at approximately 10°, was the highest amongst all the investigated cases. We show the wind direction at the metmast and the WT1 turbine heading in Figure 5. Here the toggler value of 1 indicates when the measurements were recorded for analysis. During the time of measurements, the wind direction ranged from 208° to 223°. This comparatively large variability in wind direction during measurements could be the most possible explanation influencing the spatial wind field distribution over the individual scans, and therefore the averaged results. We have added the following text to the modified manuscript:

It is noted that for the positive offset case, the spatial distribution of the  $u$  component seems to move near the rotor axis instead of deflecting towards  $y/D > 0$ . This could be potentially attributed to the 10° misalignment between the wind direction and the turbine orientation direction in addition to the large variability of the wind direction from 208° to 223° which was the highest of all investigated cases.

## Minor Comments

---

**Comment 1** — Line 5. Please change the "The measurements were conducted with..." with "The measurements were acquired by..."

**Reply:** We have changed this in the revised manuscript.

**Comment 2** — Lines 96 – 97: Please add in this sentence that WT1 is the upstream wind turbine and WT2 is the downstream.

**Reply:** We have changed this in the revised manuscript.

The upstream and downstream turbines are abbreviated as WT1 and WT2 respectively..

**Comment 3** — Line 103: Please replace the verb "outfit" with the verb "equip"

**Reply:** We have changed this in the revised manuscript.

**Comment 4** — Lines 104-105: Please add the names of the Thies products.

**Reply:** We have added the following to the text:

Inflow conditions were measured by a met mast placed  $2.6 D$  north of WT1, equipped with two anemometers, Thies First Class Wind Transmitter anemometer of type 4.3352.00.400 from at the lower tip of 54 m and close to the WT1 hub height of 116m. A wind vane of type Thies First Class Wind Direction Transmitter of type 4.3151.00.212 is also installed at 112 m.

**Comment 5** — Line 140: What is meant with the "Without generalisation ..."? Please clarify.

**Reply:** We have used the terminology without generalisation to indicate that our assumption of a vanishing vertical component might not be the only way to reconstruct two-dimensional wind fields from dual lidar measurements.

**Comment 6** — Line 167: Remove the dot after "Table"

**Reply:** Removed.

**Comment 7** — Line 168: Table 1. Label: Is it Fig. 2(b) or Fig. 2(a)?

**Reply:** The reference is for Fig. 2(a). We have made the change in the revised manuscript.

**Comment 8** — Line 183: Figure 4. Replace "The doted lines..." with "The dashed lines..."

**Reply:** Replaced.

**Comment 9** — Line 187: Please delete the second "averaging"

**Reply:** The repetition has been deleted.

**Comment 10** — Line 252, Table 3. Please add a description of each column in the label of the table.

**Reply:** We have added the following to the caption:

Summary of the measurement cases. Each case is characterised by its freestream wind speed  $u_\infty$ , turbulence intensity (TI), mean wind direction ( $\theta_{\text{wdir}}$ ), stability parameter ( $z/L$ ), stability, wind veer ( $\gamma$ ), vertical wind shear ( $\alpha_{\text{shear}}$ ) and the yaw offset of the turbines ( $\gamma_{\text{WT}}$ ).

**Comment 11** — Line 317. Replace Figure 7 with Fig. 7

**Reply:** Replaced.

**Comment 12** — Line 325. Replace Figure 7 with Fig. 7

**Reply:** Replaced.



---

## Reviewer 2

This paper presents some unique results of dual-Doppler retrieval of wind field in the induction zone of a turbine subject to different wake conditions. This work is novel and quite relevant, but some important changes, especially to the physical explanations provided to the observed phenomena, are necessary.

*We thank the reviewer for their critical assessment of our work. In the following, we address the concerns point by point. We hope these changes will positively benefit the manuscript. Comments to the reviewer points are made in blue while modifications to the manuscript are made in red.*

Based on the comments of Reviewers 1, 2 we have summarised the major changes in the revised manuscript below:

- Expanded the site characterisation section with the topography and the presence of flow blockage (treeline) in between the two turbines and the discussion section to include the effects of the topography and treeline as a possible explanation for our measured flow features and a discussion on how to decouple the terrain effects from the rotor aerodynamic effects.
- Updated the LES results section with an analysis of the statistical uncertainty of the measurements.
- Expanded the LES Results section to include the rationale behind our assumption of the vertical velocity on the Standard Uncertainty Propagation (SUP) and its impact on the width of error bars. The discussion section has been updated to include the significance of our results based on the SUP assumptions and suggestions for future measurements with a third synchronised lidar.
- The conclusion section has been reworked substantially to include a description of our measurements, measured flow features, a summary of the uncertainty analysis and summary of challenges in conducting field measurements for obtaining validation data for numerical models.

---

## General Comments

**Comment 1:** The error analysis is very accurate but some results of it may be misrepresented. SUP and LES do not include all the sources of error, as correctly indicated in Table 2. This should be reiterated when commenting, for instance, Fig. 9 to make sure the reader does not interpret the error bands based on SUP as an estimate for the limits of the difference of the LES validation. For instance, the error band around  $v$  is significantly larger than the difference shown by LES but simply due to the lack of pointing accuracy in LES.

**Reply:** Indeed, SUP and LES does not contain all sources of errors, which is why we had used both methods for our analysis. In the revised manuscript, we have clearly specified the method through with

the error bars were obtained and expanded the discussion accordingly.

We have added the similar text to the revised manuscript in Section 3.1.2 to the measurement cases. The error bars around the  $v$  component profiles are larger than the differences in the LES and WindScanner resolved profiles due to the inclusion of multiple error terms in the SUP.

**Comment 2:** Also, not including statistical uncertainty in the following plot may be misleading as this last contribution can easily dominate the overall uncertainty in real experimental campaigns. Statistical uncertainty and convergence are discussed in Section 2.3.2 but the simple comparison with the work of Simley et al. 2016 is not sufficient to justify the current results. The statistical uncertainty is a function of the specific flow conditions (mostly turbulence intensity and integral timescale) as well as number of samples. Please add at least an estimate of the error on the mean to make sure it is ok to neglect it compared to the other uncertainties.

**Reply:** We agree with the reviewer that the statistical uncertainty needs to be presented. While the total propagated uncertainty regards the accuracy of single input variables, the statistical uncertainty quantifies the precision of the results from different scans. A higher number of scans typically reduces measurement noise from the statistical error. To quantify the statistical uncertainty, we use the margin of error estimated in the scanning area, for the LES case with two aligned and operational turbines. The margin of error was calculated as  $e_{u,stat} = \frac{z_\gamma \sigma_u}{\sqrt{N_s}}$  and  $e_{v,stat} = \frac{z_\gamma \sigma_v}{\sqrt{N_s}}$ . Here  $z_\gamma$ , the confidence level, is set to 1.96, denoting the 95 % confidence interval,  $\sigma_u, \sigma_v$  are the standard deviations of the longitudinal and lateral velocity components in the scan plane obtained from the WindScanner simulations and  $N$  is the number of samples.

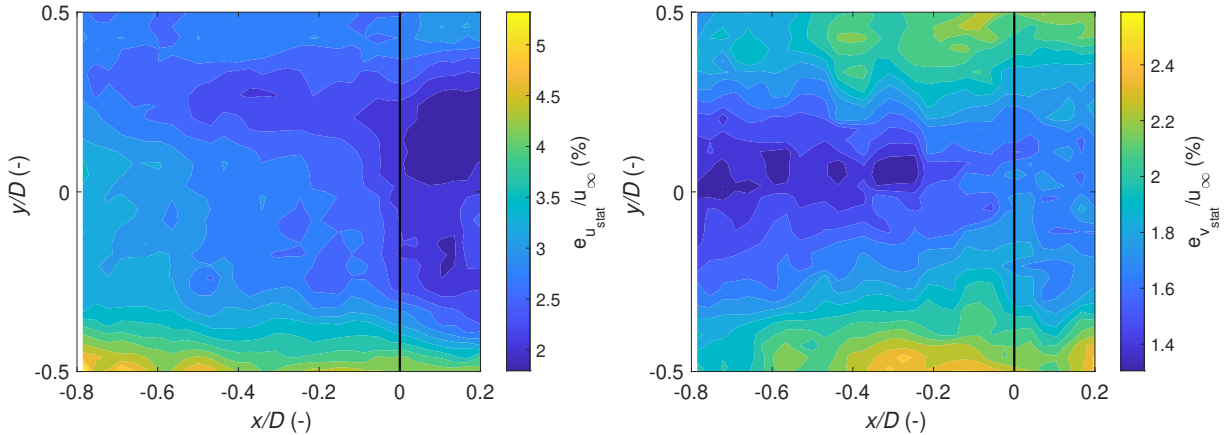


Figure 6: Statistical Uncertainty estimated for the  $u, v$  components.

Figure 6 shows the variation of the margin of error in the scanning area for the two reconstructed components normalised with the mean longitudinal wind speed. The margin of error for the longitudinal component varies in the scan area between 2 % to 5 % depending on the turbulence intensity in the wake. Similarly, for the  $v$ - component, the margin of error varies between 1.3 % and 2.5 %. The higher errors at scan edges could be attributed to the low amount of data points in these locations as a consequence of the scanning patterns. This indicates that our set-up can capture the averaged

velocities in the scan plane with a statistical uncertainty that is lower than the dual-Doppler propagated uncertainties. In the field data, we can expect that the margin of error would be slightly higher than in the idealised LES due to the filtering procedure reducing data availability in each scan.

We have added the presented analysis of the statistical uncertainty in Section 3.1 of the revised manuscript.

**Comment 3:** A major drawback is also discussing differences in the measurements that are much smaller than the associated uncertainty (e.g. Fig. 16 and 17). The claimed “asymmetries” in the yaw steering cases are not significant enough to be considered a physical feature. The uncertainty quantification must indeed be used to flag significance of the results, otherwise it becomes just a theoretical exercise. Please either mention that the observed small differences between cases 3 and 4 are not relevant (so everything is really speculative) or remove at all Fig. 16 and 17 and the associated discussion.

**Reply:** We acknowledge that we have not discussed the significance of the results in detail. We first discuss the methodology by which the error bars were drawn in Fig 16, and 17 before suggesting a way linking the uncertainty quantification exercise and the measurements.

The error bars in Figs. 14, 16, and 17 were estimated using a  $w$  component value of 1 m/s. We acknowledge that the reasoning behind the choice of  $w$  velocities for the SUP method was not detailed in the paper. In the LES analysis, the reference wind fields provided an accurate value of the local  $w$  component variation inside the scanning area. This local  $w$  velocity was subsequently used to calculate the propagated uncertainties providing a methodology to investigate the lidar error inside the LES. However, in the free field, we did not have any measurements of the local  $w$  component. Therefore, an assumption of a constant  $w$  was required for the Standard Uncertainty Propagation (SUP) methodology. For the full wake and partial wake cases, a value of  $w = 1$  m/s was assumed, similar to the wind tunnel experiments of van Dooren et al [20]. For the undisturbed inflow case, the vertical velocity would be only dominated by the temperature flux between the ground and the air, and therefore a conservative value of  $w = 0.2$  m/s was chosen based on the weakly stable conditions during the measurements.

The assumption of constant  $w$  velocities in the measurement plane for SUP calculations will have a significant impact on our results. Therefore, the errors would be overestimated at locations where the local  $w$  component would be low, for instance, the most upstream part of the scan where the aerodynamic influence of the rotor on the flow would not be felt by the wind field. To illustrate this we plot the variation of  $e_u$  and  $e_v$  in the scanning area for the LES case with an assumption of  $w = 1$  m/s in Figure 7.

The comparison of  $e_u$  and  $e_v$  for the two methods indicates two things. Firstly, assuming constant  $w$  on the scanning area masks the velocity reconstruction error that is dependent on the flow dynamics, especially close to the rotor. Secondly, the magnitude of  $e_u$  and  $e_v$  for the constant  $w$  velocity case is substantially larger than the errors estimated using the local  $w$  velocities. The consequence of this is that the presented error bars in Figures 11, 14, 16 and 17 of the original manuscript are conservative, leading to difficulties in the interpretation and significance of the results. Had the  $w$  component been low, the error bars could have been smaller and we could have made definitive statements on the significance of the results. In the revised version of the paper, we have shown and discussed the spatial variation of the propagated error using the actual and assumed vertical velocities to bridge the LES and the field measurements. We have extended the discussion section, highlighting the assumption and its impact on the significance and interpretation of the measurements. A possible workaround would have been to use a third synchronised lidar that would eliminate the assumption of vanishing vertical velocity, however,

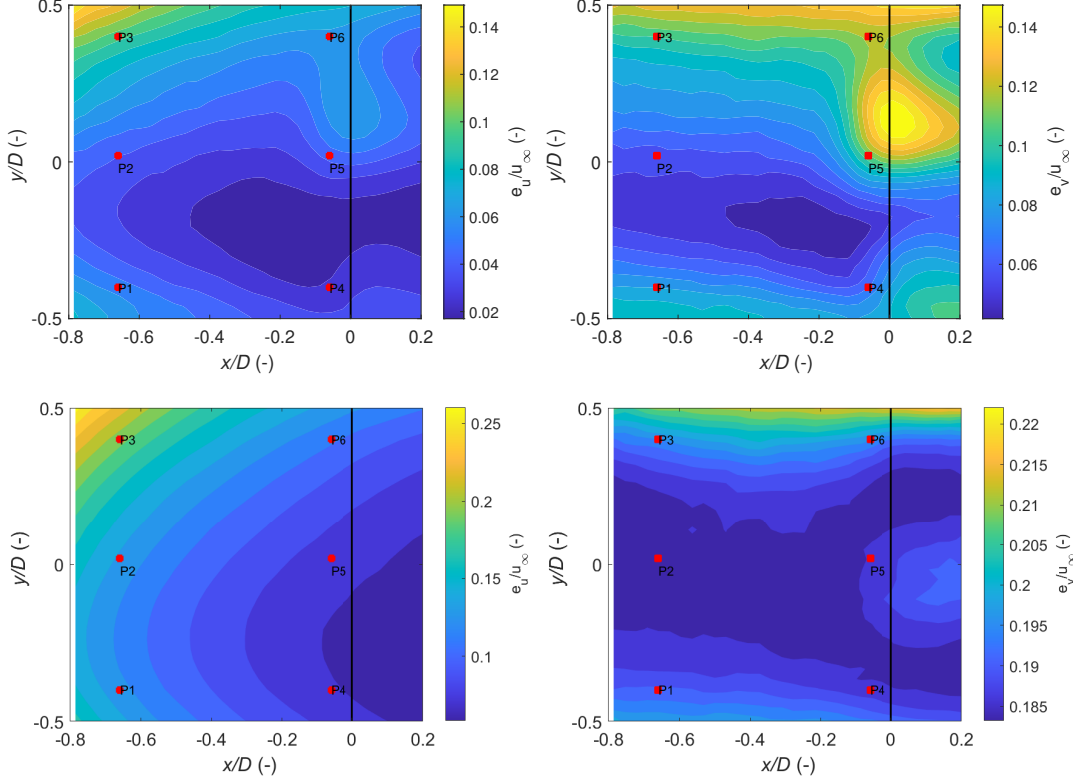


Figure 7: Variation of  $e_u$  and  $e_v$  in the scanning area using the assumption of  $w = 1$  m/s (bottom row) and the local  $w$  component from the LES (top row).

a third system was not available for measurements. We acknowledge this unavoidable limitation of our measurement setup and have made the following changes in the manuscript.

We have made the following changes in the revised manuscript.

- Expanded the LES Section 3.1 with the SUP analysis based on the assumptions of  $w$  velocity instead of the true LES velocities to link the simulations and experiments.
- Extended the discussion section, highlighting the assumption and its impact on the significance and interpretation of the measurements.

**Comment 4:** A major issue with the interpretation of the results concerns the observer asymmetry of the induction zone. First, a mild asymmetry seems to show in the LES results, but on the other side of the rotor (Fig 6) compared to the lidar observation. Please explain why this is the case. Second and foremost, the physical explanation provided for this asymmetry, namely the “different angles of attacks” between the left and right side of the rotor induced by “wind shear” is not clear. If we consider the same height AGL, then the incoming wind speed is the same on both sides of the rotor. Being the rotational speed the same, this results in identical local inflow, relative speed and angle of attack. Furthermore, it was not found any evidence in the cited references supposedly reporting such effect. The cited papers do indeed show symmetrical induction zones

even with shear, as it should be. If there's a fundamental mechanism creating this asymmetry, please provide a schematic with the angles of attacks as a function of the blade position.

**Reply:**

In our attempt to explain the measurements, we first will discuss the quality of the collected data and then proceed with an explanation for the measurement results. We are confident in the ability to achieve the scanning trajectories with high accuracy through extensive wind tunnel and field testing. Therefore, we could eliminate any mechanical/optical issues with the lidars that would contaminate measurements.

We referred to the work of Bastankah et al [2] who conducted wind tunnel measurements of a model wind turbine under sheared conditions ( $\alpha = 0.17$ ). They noted "a slight lateral asymmetry with respect to the rotor axis" visualised through iso-velocity contours at far upstream positions. Similar to our measurements, the asymmetry also disappears closer to the rotor plane. Bastankah et al provided a possible explanation of the slight asymmetry due to rotor blades experiencing different angles of attack as they move through the sheared flow. However, as pointed out, indeed the induced velocities for a rotor with a constant rpm will be the same on either side of the rotor and will only change the induction in the vertical direction. This is the effect that we wanted to describe with the work of Frosting et al [12] who show the variation of induction in the rotor plane for strongly sheared flow. We also described the mechanism of momentum transfer between the lower and upper parts of the rotor as an additional explanation for the asymmetry. The authors thank the reviewer for pointing us towards the work of Madsen et al [11] who provided similar reasoning of the wake rotation and its impact on the induced velocities at the rotor plane.

However, as noted by Reviewer 1, we had not fully characterised the test site in terms of terrain which could provide additional explanation for the measured asymmetry. The induction zone behaviour can be mischaracterised with observations if the effects of nonuniform terrain on the flow are not carefully considered. This non-uniformity could be a result of the changing terrain upstream of the turbine or the presence of a forest or a tree line. For instance, Mikkelsen et al., [13] in their dual-WindScanner lidar measurements at the DTU Riso site measured a vertical velocity of 1 m/s in the induction zone which was attributed to the upward sloping terrain upstream of the turbine.

We first discuss the layout of the site more in detail, as illustrated in Fig. 8, with a spatial resolution of 200 m obtained from [3]. While the elevations at WT1 and WT2 are similar, abrupt changes in elevation are seen upstream notably the presence of a small hill with an elevation of 105 m 22 D upstream of WT1 along the predominant wind direction, creating a slope of  $1.09^\circ$  towards the two turbines. We also note the presence of a village, tree lines and small clumps of forested terrain along the predominant wind direction. Furthermore, a treeline exists between WT1 and WT2 and therefore in the induction region of WT2. The treeline extended towards the met mast with a height of approximately 15 m-20 m estimated from pictures taken during the installation campaign. Further analysis of the measurements from the same site was done by Hulsman et al. [10] who showed a clear effect of the same tree line by comparing the met mast and the VAD lidar data at 100 m AGL. However, the comparison is not directly transferable in our sector of interest due to the orientation of the VAD lidar and the met mast but provides enough evidence of the perturbation of the flow by the treeline. This is consistent with literature where trees acting as windbreaks have been shown to perturb the vertical flow profile high above the treeline [7, 19].

We believe that the effect of terrain and in particular treeline could have influenced the flow behaviour in the induction zone, which we did not address previously. Furthermore, these effects could have also impacted the WindScanner measurements, in particular, the assumption of vanishing vertical wind speed

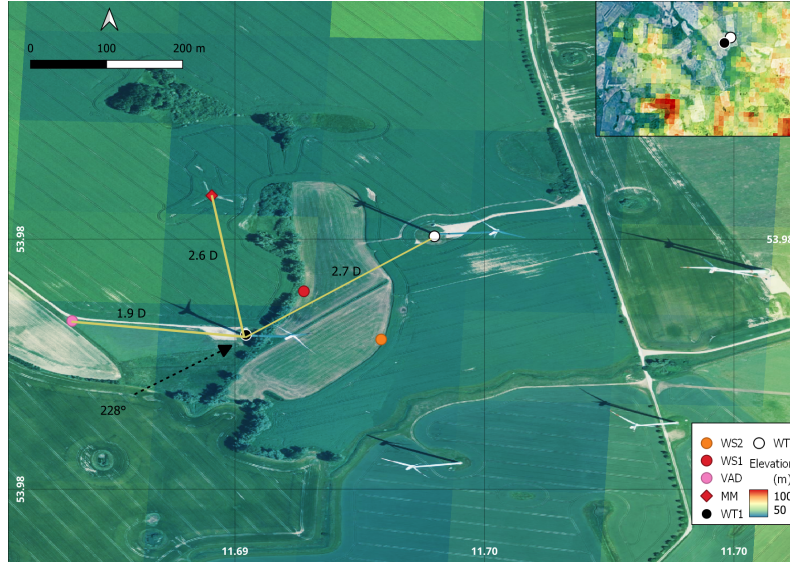


Figure 8: The wind park and measurement layout at Kirch Mulsow overlaid with elevation contours. A zoomed-out image of the site is shown in the top right corner illustrating the hills present upstream of the wind park. Here WT1, and WT2 refer to the upstream and downstream turbines, MM and VAD refer to the met mast and the inflow lidar while WS1 and WS2 refer to the two WindScanners.

for the dual-Doppler reconstruction which could have influenced the measurement results.

In our present setup, we could not quantify the magnitude of these terrain effects on the flow and the lidar measurements. We could not acquire measurements when both the turbines were non-operational, which would have provided insights into the flow behaviour due to terrain and the tree line. Using a high-resolution LES with a terrain map could have been used to isolate the terrain influences. However, the LES runs in our study were intended to study the lidar measurement accuracy and therefore were initialised with a roughness length as a proxy for the terrain complexity and hence not fully representative of the site. This could explain why the asymmetry exists on the other side of the rotor compared to field measurements.

We hope that these changes to the manuscript will provide a suitable explanation for the measurements.

We have updated the test site description with the terrain map and described the treeline in between WT1 and WT2 and added the terrain and treeline effects as a possible additional effect for the flow perturbation in all the sections. We have further updated the discussion section with the effect of the terrain on the flow and the dual-Doppler reconstruction and discussed the limitation of our simulation set-up where the terrain and hence the lidar error due to terrain could not be modelled.

## Specific Comments

---

**Comment 1** — L 18, "...due to the extraction of kinetic energy by the rotor": this may be

a subtlety but technically induction zones are present also around bodies that do not necessarily extract significant kinetic energy from the flow (e.g. in front of an airfoil). It is suggested rephrasing as “. . . due to the rotor thrust”.

**Reply:** The sentence has been rephrased as suggested.

**Comment 2** — L 57: please clarify what “assumptions of the global flow field” refers to.

**Reply:** The assumption of global flow field refers to the assumption of a constant vertical wind component required to perform the dual-Doppler reconstruction. We have replaced the phrasing in the paper. However, owing to the lidar measurement principle and scanning limitations, such as the volume averaging effect, assumptions of vertical velocity for dual-Doppler reconstruction, scanning speeds, beam pointing, and intersection accuracies, a thorough error and uncertainty assessment is required before interpreting the measurements

**Comment 3** — Table 2: A few improvements are suggested:

- The source of the dual-Doppler error is not necessarily “Non-ideal lidar placement impacts the beam-intersection angles” as an ideal placement leading to 0 error does not exist. It is indeed an “Amplification of single-Doppler uncertainty due to dual-Doppler reconstruction”. We have changed the text in the revised manuscript.
- The “averaging period error” could be renamed “statistical uncertainty”. We have changed the text in the revised manuscript.
- It would be better to remove the “unavoidable” word in the description of the error due to neglecting  $w$ . In fact, one could use for instance continuity or other techniques to estimate  $w$ . Also, please explain SUP in the caption. We have changed the text in the revised manuscript.

**Reply:** We have changed the descriptions of the errors to reflect the reviewer comments and defined the abbreviations of LES and SUP on the caption.

**Comment 4** — L 213: Please add reference for the dual-Doppler error (e.g. Stawiarski 2013). Also, the  $\Delta\chi$  which indicates the angle between the intersecting beams which is the driving factor for the error is not the difference of the azimuth angles  $\chi_1 - \chi_2$ . Please clarify this point and possibly use a symbol other than  $\Delta\chi$  to describe the intersection angle as  $\chi$  was already used for azimuth.

**Reply:** We have added references to Stawiarski et al [18], van Dooren et al [22] and Pena and Mann [?] as appropriate references here. Indeed, we refer here to the intersection angle of the beams which scales the dual-Doppler reconstruction error as described in Stawiarski et al [18]. We have represented the term as  $R_{\text{int}}$  in the revised manuscript.

**Comment 5** — Table 3: A few improvements are suggested:

- Please explain all symbols in the caption.



- The stability classes indicated here do not match the three given later (stable, neutral, unstable)
- Add  $z/L$  in a new column

**Reply:**

- We have expanded the caption to the following:  
Summary of the measurement cases. Each case is characterised by its freestream wind speed  $u_\infty$ , turbulence intensity (TI), mean wind direction ( $\theta_{\text{wdir}}$ ), stability parameter ( $z/L$ ), stability, wind veer ( $\gamma$ ), vertical wind shear ( $\alpha_{\text{shear}}$ ) and the yaw offset of the turbines ( $\gamma_{\text{WT}}$ ).
- The table has been expanded to contain  $z/L$  values and the stability classes has been checked and made consistent with the results section.

**Comment 6** — L 254-259: Please add justification or reference for the choice the stability classes based on  $L$ .

**Reply:** For justification of the choice of  $L$  for stability classification, we have added the following references to the text: .

The atmospheric stability of the boundary layer can be characterised by the Monin-Obhukov similarity theory [14, 1]. The stability parameter  $z/L$  was measured by the eddy covariance station at a height of 6 m above the ground following Bromm et al,[6].

**Comment 7** — L 325-327: The details of the SUP calculation should be moved at L 314 when first introducing the figures.

**Reply:** We have moved the details of the SUP calculation before the figures are introduced.

**Comment 8** — L 331-332: Please expand further why a high elevation leads to a high uncertainty associated with elevation. Is this just due to the structure of  $\frac{\partial u}{\partial \delta}$  being proportional to  $\delta$ ?

**Reply:** The general form of the uncertainty propagation involves the product of the partial derivative and the uncertainty of the input variable, in this case, line-of-sights, beam pointing angles and vertical wind component. For the case of the elevation angle, the partial derivative  $\frac{\partial u}{\partial \delta}$  was positively correlated to the elevation angle  $\delta$ . Therefore, an increase in  $\delta$  would result in a more substantial impact on the overall uncertainty in the wind component  $e_u$ . We have modified the text to the following:

At P1, P2 and P3,  $e_{\delta_i}$  is the largest contributor due to the severe elevation angles required to scan at these points and the positive correlation between  $\frac{\partial u}{\partial \delta}$  and  $\delta$ .

**Comment 9** — L 332-333: It is also not immediately clear why the error due to neglecting  $w$  is larger for the lidar more aligned with the wind. Please clarify.

**Reply:** We can explain this from the contribution of the vertical velocity to the individual line-of-sight of the two lidars. For the un-aligned lidar, the lidar measures with an angle to the measurement point and therefore the line-of-sight component will contain contributions from both the lateral and vertical

velocity components. Neglecting the vertical velocity might have a smaller impact on this lidar since it already incorporates both components in its measurements. For the aligned lidar, the measurements are more sensitive to the changes in the  $w$  component. For a non-zero  $w$  component, the aligned lidar will contain a larger contribution of the  $w$  component projected onto its line-of-sight compared to the un-aligned case. We have modified the text to the following:

The varying contributions of  $e_{w,i}$  at the points of interest can be explained by the relative alignment of the lidar with the wind direction. For a non-zero  $w$  component, an aligned lidar will contain a larger contribution of the  $w$  component projected onto its line-of-sight compared to the un-aligned case.

**Comment 10** — L 333-334: Not only P3 and P6, but also P5 has a preponderant error  $e_{w,1}$  which should be explained.

**Reply:** The error at P5 follows the same argumentation as Comment 9 and is dominated by the term  $e_{w,i}$ . The value of  $e_{w,1}$  is larger than P3 and P6 due to the large local  $w$  velocity close to the rotor obtained from the LES (Fig. 6 (top right)). We have modified the text to the following:

Similarly, at P3, P5 and P6, WS1 is approximately aligned with the longitudinal wind speed component. So the errors at these points are dominated by the  $e_{w,1}$ , which is highest at P5 due to the large local  $w$  velocity in the LES field (Fig. 06 (top right)).

**Comment 11** — L 341: The location  $x/D = 0.16$  is not shown in Fig 9.

**Reply:** Thank you for pointing this out. We have corrected the location in the text to  $x/D = -0.08$  as depicted in Fig. 9.

**Comment 12** — L360-361: There are several ways stable stratification could impact the induction strength, please explain why it is enhancing the velocity decrease in this case.

**Reply:** Stable stratification inhibits wind vertical turbulent mixing. In the induction zone, where the rotor blades are influencing the flow, stable stratification can limit the upward transport of momentum. This reduced mixing can lead to an enhancement of the induction zone and the velocity decrease. We have modified the text to the following:

This strong velocity deficit can be attributed to high axial induction and weakly stable stratification during the measurement period inhibiting vertical turbulent mixing.

**Comment 13** — L367-368: It is not clear why the blades would experience different relative inflow on the left and right side of the rotor. Considering hub-height for simplicity, the inflow velocity  $u_{hub}$  is the same on both sides of the rotor if vertical shear only is present. Being the rotational component  $\omega R$  necessarily the same, the velocity experienced by the blades is identical. Also, the cited reference by Meyer-Forsting shows a symmetrical behavior of the induction in their LES results (below) and is therefore inadequate. The explanation based on the interaction of wake rotation and shear is sounder [Madsen et al., 2014] at least in the near wake. Please clarify this point.

**Reply:** We have addressed this point in General Comment 4. Indeed the induced velocities for a rotor with a constant rpm will be the same on either side of the rotor and will only change the induction in the vertical direction. This is the effect that we wanted to describe with the work of Frosting et al [12] who show the variation of induction in the rotor plane for strongly sheared flow. We have added a further explanation of the asymmetry due to terrain effects and the presence and influence of a treeline in between WT1 and WT2.

Looking downwind, this slight asymmetry could be attributed to the presence of a tall treeline in-between WT1 and WT2 perturbing the flow and the strong vertical shear  $\alpha_{\text{shear}} = 0.21$  that causes a vertical wind speed gradient varying the relative wind speed and the angle of attack of the blades during a rotation. Additionally, the induced velocities at the rotor plane are influenced by the counter-rotating wake creating a momentum transfer between the lower and upper rotor regions leading to a difference in flow magnitude between  $y/D > 0$  and  $y/D < 0$  [11]. Hence, the blade sections would experience varying blade forces that vary the local thrust coefficient, and hence, the induction factor and corresponding deceleration.

**Comment 14** — L 380: Is the vertical velocity used only to compute uncertainty or also for the dual-Doppler reconstruction? Please explain.

**Reply:** The vertical velocity assumption of 0.2 m/s was chosen only for computing the uncertainty while the dual-Doppler reconstruction was done by assuming  $w = 0$  m/s. Similarly, for the uncertainty assessment for the partial and full wake cases, a constant vertical velocity of 1 m/s was assumed following the work of van Dooren et al [20]. The implications of this assumption on the propagated uncertainty has been discussed in Major Comment 3. We have modified the text to the following:

For calculating the propagated uncertainties, a constant vertical component  $w = 0.2$  m/s is assumed, as no wakes propagating from the non-operational upstream turbine and no direct measurements of the  $w$  component were available in the scanned area.

**Comment 15** — L 388: Please clarify what the  $1-96\sigma$  bounds mean. Is this the uncertainty from SUP? Why is the error bar not centered on the data?

**Reply:** We clarify that the error bars presented represent the propagated uncertainties from SUP and not the statistical uncertainty. The revised version of the manuscript has been updated with a plot with centred error bars on the WindScanner data.

**Comment 16** — Figure 12: A deeper analysis on why FLORIS is underpredicting so drastically the induction is needed. The fact that even at the rotor plane the estimated induction is 1/3 that of other models sounds concerning. Please also provide the Ct for this case to allow other researchers to replicate the results.

**Reply:** We acknowledge that the systematic underprediction of the velocity deceleration's from the FLORIS model is a cause of concern and hence was not used for estimating the velocity decelerations in the partial and full wake cases. We had used the FLORIS+Induction coupling described in Branlard et al [5] that downloaded from the Github repository. We also contacted the authors of the paper [5] to describe and find a solution to the problem. The most likely reason for the discrepancy is a bug in the coupling between the induction zone models and the wake models in FLORIS. This reasoning is

supported by the good agreement between the standalone induction zone models that are used in the coupling and the field measurements.

Due to an NDA with the turbine operator, we cannot disclose the turbine Ct curve for confidentiality.

**Comment 17** — L 431: Same as comment on L 380.

**Reply:** Please refer to Comment 14 for our answer.

**Comment 18** — L 440: It is unclear what “profiles at  $y/D \pm 0.5$ ” means as those specific spanwise locations correspond to a point value in the velocity deficit, not “profiles”.

**Reply:** We apologise for the ambiguity. We have rephrased the sentence to:  
Interestingly, the spanwise velocity profiles at various upstream positions exhibits a slight asymmetry.

**Comment 19** — L 442: The concept of “asymmetric induction” here is repeated and not explained. Again, the cited references do not mention any asymmetric induction but focus on the effects of stability and veer on the wake morphology.

**Reply:** We have removed the term “asymmetric induction zone” as the reference stated are primarily discussing the wake shape under wind veer and shear.

**Comment 20** — L 453-456: You could cite Fleming et al, 2018 to support the fact that wake rotation and counter-rotating vortices sum up in the positive yaw case and cancel out in the negative one.

**Reply:** We have added reference to Fleming et al.,2018 and modified the text to the following:

The findings correspond to Fleming et al.,2018, where a stronger wake deflection for positive yaw case is seen due to the aggregated effect of the wake rotation and counter-rotating vortices in comparison to the negative deflection case.

**Comment 21** — L 457: Which velocity? The lateral one?

**Reply:** Here we refer to the longitudinal velocity and have modified the text accordingly.

**Comment 22** — Figures 16 and 17: please swap the plots to show first the positive yaw as in Figure 15.

**Reply:** We have swapped the plots to maintain consistency with Fig. 15.

**Comment 23** — L 474-475: It is hard to see the claimed stronger induction for negative y. Maybe provide a quantitative parameter like the velocity ratio between inflow and location closer to rotor plane.

**Reply:** We estimated the velocity reduction between the most upstream scan location ( $0.8 D$ ) and very close to the rotor plane ( $0D$ ) by calculating the velocity ratio between the two locations at various spanwise locations given by the following equation:

$$v_{\text{ratio}} = \frac{v_{0.8D}}{v_{0D}} \quad (1)$$

For brevity, we show the velocity reduction ratio at spanwise positions  $y/D = 0.19$  and  $y/D = -0.19$  as the trend remained similar towards the rotor tips. For the positive yaw case, the value of  $v_{\text{ratio}}$  was 1.2 and 1.14 at  $y/D = -0.19$  and  $y/D = 0.19$  respectively. Similarly, for the negative yaw case, the value of  $v_{\text{ratio}}$  was 1.23 and 1.04 at  $y/D = -0.19$  and  $y/D = 0.19$  respectively. We have added the following text to the revised manuscript:

The induction strength between the left and right sides of the rotor is quantified using the ratio of the longitudinal wind speed far upstream of the scan at  $0.8 D$  and the rotor plane at  $0 D$  as  $v_{\text{ratio}} = \frac{v_{0.8D}}{v_{0D}}$ . For the positive yaw case, the value of  $v_{\text{ratio}}$  was 1.2 and 1.14 at  $y/D = -0.19$  and  $y/D = 0.19$  respectively. Similarly for the negative yaw case, the value of  $v_{\text{ratio}}$  was 1.23 and 1.04 at  $y/D = -0.19$  and  $y/D = 0.19$  respectively with similar trends observed at other spanwise positions.

**Comment 24** — L 477-478: The wake recovery followed by the deceleration is only visible for the positive yaw case.

**Reply:** We regret that our statement on the paper has been misinterpreted. We have not noted that the wake recovery followed by deceleration was visible in the positive yaw case. We simply wanted to convey that the induction effect is stronger at  $y/D < 0$  which was exposed to the wake for the negative yaw case. We have added the following text to the revised manuscript:

For the negative offset case, similar effects of the induction are seen where the wake at  $y/D < 0$  decelerated faster compared to the freestream at  $y/D > 0$ .

**Comment 25** — L 496: why is the probe averaging not included as possible source of errors?

**Reply:** Probe volume averaging is indeed a source of error and we have added this in the revised version.

**Comment 26** — L511 - The explanation of the angle of attack as the cause of non-symmetrical induction is not sound (see above). The cited Bastankhah paper shows a symmetrical induction for 0-yaw misalignment (below):

**Reply:** Bastankah et al [2], in their measurements of a turbine operating with zero yaw noted "a slight lateral asymmetry with respect to the rotor axis" visualised with the iso-velocity contours at far upstream positions ( $x/D \approx 1$ ) with the asymmetry vanishing towards the rotor plane, similar to our measurements.

We have updated the explanation of the non-symmetrical induction to also include the interaction of wind shear with wake rotation and the effect of terrain and the tall tree line.

**Comment 27** — L 524-525: the non-symmetrical induction one is hard to see (see above).

**Reply:** The non-symmetrical induction for the aligned inflow case is visible through the iso-velocity contours at far upstream locations ( $x/D \approx 1$ ) and disappears towards the rotor plane.

**Comment 28** — L 550: the explanation of the shear as the cause of non-symmetrical induction is not sound (see above).

**Reply:** We have updated the explanation of the non-symmetrical induction to also include the interaction of wind shear with wake rotation and the effect of terrain and the tall tree line. We hope that these changes to the manuscript will provide a suitable explanation for the measurements.

## References

- [1] R. J. Barthelmie. The effects of atmospheric stability on coastal wind climates. *Meteorological Applications*, 6(1):39–47, 3 1999.
- [2] M. Bastankhah and F. Porte-Agel. Wind tunnel study of the wind turbine interaction with a boundary-layer flow: Upwind region, turbine performance, and wake region. *Physics of Fluids*, 29(6), 2017.
- [3] BKG. Digitales Geländemodell Gitterweite 200 m, 2013.
- [4] A. Borraccino, D. Schlipf, F. Haizmann, and R. Wagner. Wind field reconstruction from nacelle-mounted lidar short-range measurements. *Wind Energy Science*, 2(1):269–283, 5 2017.
- [5] E. Branlard and A. R. Meyer Forsting. Assessing the blockage effect of wind turbines and wind farms using an analytical vortex model. *Wind Energy*, 23(11):2068–2086, 11 2020.
- [6] M. Bromm, A. Rott, H. Beck, L. Vollmer, G. Steinfeld, and M. Kühn. Field investigation on the influence of yaw misalignment on the propagation of wind turbine wakes. *Wind Energy*, 21(11):1011–1028, 11 2018.
- [7] J. Counihan, J. C. Hunt, and P. S. Jackson. Wakes behind two-dimensional surface obstacles in turbulent boundary layers. *Journal of Fluid Mechanics*, 64(3):529–564, 1974.
- [8] R. Frehlich. Effects of wind turbulence on coherent Doppler lidar performance. *Journal of Atmospheric and Oceanic Technology*, 14(1):54–75, 1997.
- [9] A. Giyanani, M. Sjöholm, G. Rolighed Thorsen, J. Schuhmacher, and J. Gottschall. Wind speed reconstruction from three synchronized short-range WindScanner lidars in a large wind turbine inflow field campaign and the associated uncertainties. *Journal of Physics: Conference Series*, 2265(2):022032, 5 2022.
- [10] P. Hulsman, C. Sucameli, V. Petrović, A. Rott, A. Gerds, and M. Kühn. Turbine power loss during yaw-misaligned free field tests at different atmospheric conditions. *Journal of Physics: Conference Series*, 2265(3):032074, 5 2022.
- [11] H. A. Madsen, V. Riziotis, F. Zahle, M. O. Hansen, H. Snel, F. Grasso, T. J. Larsen, E. Politis, and F. Rasmussen. Blade element momentum modeling of inflow with shear in comparison with advanced model results. In *Wind Energy*, volume 15, pages 63–81. John Wiley and Sons Ltd, 1 2012.
- [12] A. R. Meyer Forsting, M. P. Van Der Laan, and N. Troldborg. The induction zone/factor and sheared inflow: A linear connection? In *Journal of Physics: Conference Series*, volume 1037, page 072031. IOP Publishing, 6 2018.
- [13] T. Mikkelsen, M. Sjöholm, P. Astrup, A. Peña, G. Larsen, M. F. van Dooren, and A. P. Kidambi Sekar. Lidar Scanning of Induction Zone Wind Fields over Sloping Terrain. *Journal of Physics: Conference Series*, 1452(1):012081, 1 2020.

- [14] A. S. Monin and A. M. Obukhov. Basic laws of turbulent mixing in the surface layer of the atmosphere. *Originally published in Tr. Akad. Nauk SSSR Geophys. Inst*, 24(151):163–187, 1954.
- [15] A. T. Pedersen and M. Courtney. Flywheel calibration of a continuous-wave coherent Doppler wind lidar. *Atmospheric Measurement Techniques*, 14(2):889–903, 2 2021.
- [16] A. Peña and J. Mann. Turbulence Measurements with Dual-Doppler Scanning Lidars. *Remote Sensing*, 11(20):2444, 10 2019.
- [17] M. Sanchez Gomez, J. K. Lundquist, J. D. Mirocha, R. S. Arthur, D. Muñoz-Esparza, and R. Robey. Can lidars assess wind plant blockage in simple terrain? A WRF-LES study. *Journal of Renewable and Sustainable Energy*, 14(6):63303, 11 2022.
- [18] C. Stawiarski, K. Traumner, C. Knigge, and R. Calhoun. Scopes and challenges of dual-doppler lidar wind measurements—an error analysis. *Journal of Atmospheric and Oceanic Technology*, 30(9):2044–2062, 2013.
- [19] N. Tobin, A. M. Hamed, and L. P. Chamorro. Fractional Flow Speed-Up from Porous Wind-breaks for Enhanced Wind-Turbine Power. *Boundary-Layer Meteorology*, 163(2):253–271, 5 2017.
- [20] M. F. van Dooren, F. Campagnolo, M. Sjöholm, N. Angelou, T. Mikkelsen, and M. Kühn. Demonstration and uncertainty analysis of synchronised scanning lidar measurements of 2-D velocity fields in a boundary-layer wind tunnel. *Wind Energy Science*, 2(1):329–341, 6 2017.
- [21] M. F. van Dooren, A. P. Kidambi Sekar, L. Neuhaus, T. Mikkelsen, M. Hölling, and M. Kühn. Modelling the spectral shape of continuous-wave lidar measurements in a turbulent wind tunnel. *Atmospheric Measurement Techniques*, 15(5):1355–1372, 3 2022.
- [22] M. F. van Dooren, D. Trabucchi, and M. Kühn. A methodology for the reconstruction of 2D horizontal wind fields of wind turbinewakes based on dual-Doppler lidar measurements. *Remote Sensing*, 8(10):809, 9 2016.